Electron Probe Analysis of Human Skin: Element Concentration Profiles

Ronald R. Warner, Ph.D., Mark C. Myers, B.S., and Dennis A. Taylor
Procter and Gamble Co., Miami Valley Laboratories, Cincinnati, Ohio, U.S.A.

Concentration profiles for the major biological inorganic elements Na, P, S, Cl, and K were measured across human skin using electron probe analysis and analytical electron microscopy. Determinations were made within the cytoplasm of individual cells. Uniform element concentrations were present throughout the viable tissue, whereas element profiles in the stratum corneum were considerably diverse. Phosphorus was practically absent from the stratum corneum. Sulfur (per unit volume) continuously increased from the inner to the outer cell layers of the stratum corneum largely as a result of cytoplasmic water loss as cells migrate to the surface. Potassium was essentially excluded from the inner stratum corneum. Very large gradients for K, Na, and Cl occurred from the middle of the stratum corneum to its outer surface; these gradients are likely the result of the inward diffusion of salts from sweat and could play a variety of physiological roles. The paucity of K and P within the inner stratum corneum suggests these important intracellular solutes (and perhaps others, including water) are recycled within the viable tissue, thus providing a virtual nutrient supply immediately underneath the stratum corneum. Alterations in this recirculation could have a regulatory function in the physiology of this tissue. *J Invest Dermatol 90:78–85, 1988*

The previous paper described the water concentration profile across normal human skin [1]. In this paper we report the distribution of the major biological elements Na, P, S, Cl, and K across the skin epithelium.

One of the more important functions of skin is to control the transfer of electrolytes and water across its borders. This function is common to all epithelia. Usually this epithelial function is studied by measuring fluxes, electrical parameters, and intracellular solute concentrations, and such investigations owe much to earlier (and current) studies on the skin of the frog. Considering the wealth of data available on most epithelia, and the historical and contemporary importance of the frog skin, it is surprising that comparable studies are virtually nonexistent for mammalian skin.

A relatively small number of studies exist on the handling of the major inorganic elements by mammalian skin, and these studies can be summarized quite briefly. It is known that electrolytes have a very low permeability across skin [2–5], and reflecting this low permeability, the epidermal transudate was shown to have an extremely low salt content [6,7]. Concerning the electrical properties of mammalian skin, most studies have addressed the galvanic skin response [8] or the response of skin in different moisturization states to electrical stimulation [9]. Although it has long been known that the mammalian epidermis *per se* can generate an electrical potential, only recently has this potential been shown to be due, at least in part, to an active inwardly directed sodium pump within the viable tissue similar to that in frog skin [10]. A similar active sodium pump has been demonstrated in fetal sheep and pig skin [11]. The function of this mechanism for net sodium movement in mammalian skin is not known, but proposed functions are promotion of epidermal wound healing and fetal osmoregulation [10,11].

A small literature also exists on the elemental content of mammalian skin. Surprisingly little conventional wet chemistry has been done, and most of this work has addressed S- and P-containing organic molecules. The role of S in keratinization has been studied [12,13], and the distribution of P has been investigated indirectly [14–16]; little P is presumed to be present in the stratum corneum. We are aware of only one study in which conventional techniques were used to measure the intracellular content of an electrolyte in mammalian skin; Na was measured in the fetal skin of sheep [11]. In mammalian skin, unlike other epithelia, most determinations of elemental content have used the electron microprobe. In addition to preliminary investigations [17,18], these studies have measured the distribution of the nondiffusible elements S and P [19–21] and, with the advent of recently introduced procedures, the distribution of more diffusible elements [22–25]. Less rigorous techniques have been used to visualize Ca at an ultrastructural level [26].

Diffusible elements play particularly important roles within cells. The major inorganic elements Na, K, and Cl, and the element Ca, are often mediators by which cells perform their functions, good examples being nerve transmission and muscle contraction. The regulation of cell proliferation, growth, and differentiation appears to be controlled by alterations in the intracellular levels of Na, H, K, and Ca [27–31]. Diffusible elements affect enzyme activities and protein organization [32,33], and indeed a variety of metabolic functions are highly sensitive to pH, ionic strength, and osmolyte composition [34]. Knowledge of elemental distributions within mammalian skin, particularly of diffusible elements, should provide information on how this tissue limits the fluxes of electrolytes, on the origin of skin electrical parameters, and on the normal ionic environment appropriate for enzymatic activities of this tissue. Knowledge of element distributions is a first step towards investigating the potential involvement of diffusible elements in proliferation, differentiation, and desquamation in mammalian skin and is fundamental to understanding the role of diffusible elements in skin dysfunction. In this paper we report measurements of cytoplasmic

Manuscript received March 2, 1987; accepted for publication May 14, 1987.

Reprint requests to: Ronald R. Warner, Ph.D., Miami Valley Laboratories, Procter and Gamble Co., P.O. Box 398707, Cincinnati, OH 45239-8707.

Abbreviations:
EDS: energy dispersive spectrometers
STEM: scanning transmission electron microscope

0020-202X/88/$03.50

elemental concentrations measured within individual cells throughout normal skin epithelium in the human.

An abstract of this work has been published [35].

MATERIALS AND METHODS

Sample preparation was described in the previous paper [1]. Briefly, skin was obtained from the lower leg of one healthy Caucasian male in summer and winter. In either season the skin was smooth and lustrous. No fluid of any kind was applied to the skin before biopsy. The biopsy was obtained from a wheal raised by subcutaneous injection of lidocaine (xylocaine, 2%) with epinephrine (1:100,000). A portion of the biopsy was frozen by plunging into a propane cryogen. One-micron-thick cryosections were obtained at −100°C or colder. Cryosections were placed on Formvar-covered nickel slot grids, sandwiched between a second Formvar film, and freeze-dried overnight. Sections were removed from the vacuum evaporator and analyzed immediately that day. These sample preparation procedures have been shown to preserve inorganic element distributions at the same or higher resolution than that used in this study [36–39].

Analyses were performed in the STEM (scanning transmission electron microscope) mode using a Cameca MBX electron microprobe at 45 kV or a modified [40] Hitachi H500 analytical electron microscope at 100 kV, both with Kevex 7000 energy dispersive spectrometers (EDS) [1]. Element measurements for Na, P, S, Cl, and K, and measurements for water content [1], were made simultaneously at each point. At the time of these analyses, our quantitative capabilities were not fully implemented, and results are presented simply as x-ray counts. Assuming a uniformly thick cryosection as in the preceeding paper [1], x-ray counts are directly proportional to elemental content per unit volume of tissue. We feel this is an adequate way to express data on the relative distribution of elements across the tissue.

Possible electron beam-induced mass loss was evaluated for each element in each analysis by graphically monitoring the integrated elemental x-ray count rate as a function of time [41]. To be acceptable, the x-ray count had to vary linearly with time and had to have an intercept at the origin; these conditions were usually satisfied.

A single profile from within the viable tissue to the outer stratum corneum cell was measured on each cryosection, with all measurements being made in the cellular cytoplasm. To account for variations in thickness between cryosections and for the different analysis conditions between instruments, individual element profiles were normalized for purposes of averaging. For each profile, x-ray counts for the innermost three or four stratum corneum cells were averaged and a normalization factor obtained by scaling these averages to an arbitrary value. Mean elemental content (x-ray counts) at the various analysis sites was directly determined from the normalized profiles. It could not be determined whether all stratum corneum layers were retained in a cryosection, and it is likely that some profiles were not obtained across the full thickness of this morphological region.

In some instances, elemental profiles were replotted in units of element x-ray counts/continuum x-ray counts, which is proportional to elemental content per unit dry weight [42]. For each data point, the x-ray count for an element was divided by its associated continuum measurement [1]. These element profiles were directly averaged without normalization.

RESULTS

Morphology and typical EDS spectra from freeze-dried cryosections were shown in the previous paper [1].

Specimen Storage Freeze-dried cryosections stored at room temperature for 24 h, even under instrument vacuum, occasionally suffered from formation of salt crystals and the appearance of lipid exudates. A typical example of these artifacts is shown in Fig 1. Lipid migration in freeze-dried cryosections has been observed previously [43]. Not all regions of a stored section exhibited the redistribution artifacts shown in Fig 1, and qualitative element and dry mass profiles in unaffected areas of a stored section were not noticeably different from sections analyzed immediately following freeze-drying. However, the obvious redistribution of sample constituents was sufficiently disconcerting to discourage sample storage, and all analyses reported here were from sections analyzed immediately after freeze-drying.

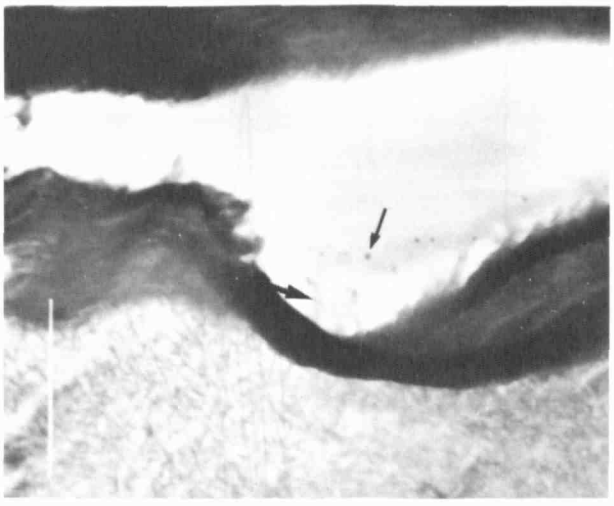

Figure 1. Artifacts after sample storage at room temperature. As seen near the center of the image, lipid has migrated from the stratum corneum onto the open support film (large arrow). Associated with this region are crystals of K and NaCl salts (small arrow, element identification not shown). Bar = 5 μm.

Element Profiles per Unit Tissue Volume Element profiles were similar whether obtained from either instrument or in skin from either season. All profiles were pooled.

Normalized profiles and the mean of these profiles are shown in Figs 2 and 3 for the (predominantly) nondiffusible elements P and S, respectively. The cellular P content (Fig 2) is relatively constant throughout the viable tissue, although often the P content appears to be elevated in the last granular cell layer. There is a precipitous drop in P to insignificant levels in the stratum corneum, and the very low P levels generally continue throughout the horny layer. As shown in Fig 2, the drop in P at the inner stratum corneum boundary is generally complete from one cell layer to the next. Usually the dramatic decrease in P occurs in what we identified as the first stratum corneum cell layer; occasionally the drop occurs just before or after this layer.

Like the P distribution, the cellular S content per unit volume (shown in Fig 3) is relatively constant throughout the viable tissue. Unlike the P distribution, there is an increase in S in the first stratum corneum layer, and S per unit volume continues to increase throughout the stratum corneum until it attains a nearly fourfold increase at the outer surface.

The profile for the diffusible element Na (Fig 4) appears similar to that for S. The Na content is relatively constant throughout the viable tissue, and increases to high levels at the outer stratum corneum cell layer. There are differences from S, however. The Na content does not immediately increase with entry into the stratum corneum, but instead continues at approximately the same level as that in the viable tissue until nearly half-way through the stratum corneum. The Na increase is then very rapid and, at the surface, achieves a sevenfold increase over the viable tissue content.

The Cl profile (Fig 5), like S and Na, is relatively constant throughout the viable tissue and increases to high levels at the stratum corneum surface. Unlike the other elements, there appears to be a jump in the Cl content at the stratum corneum-granulosum interface, and then little further change in Cl until, as observed for Na, approximately mid-way through the stratum corneum there is a

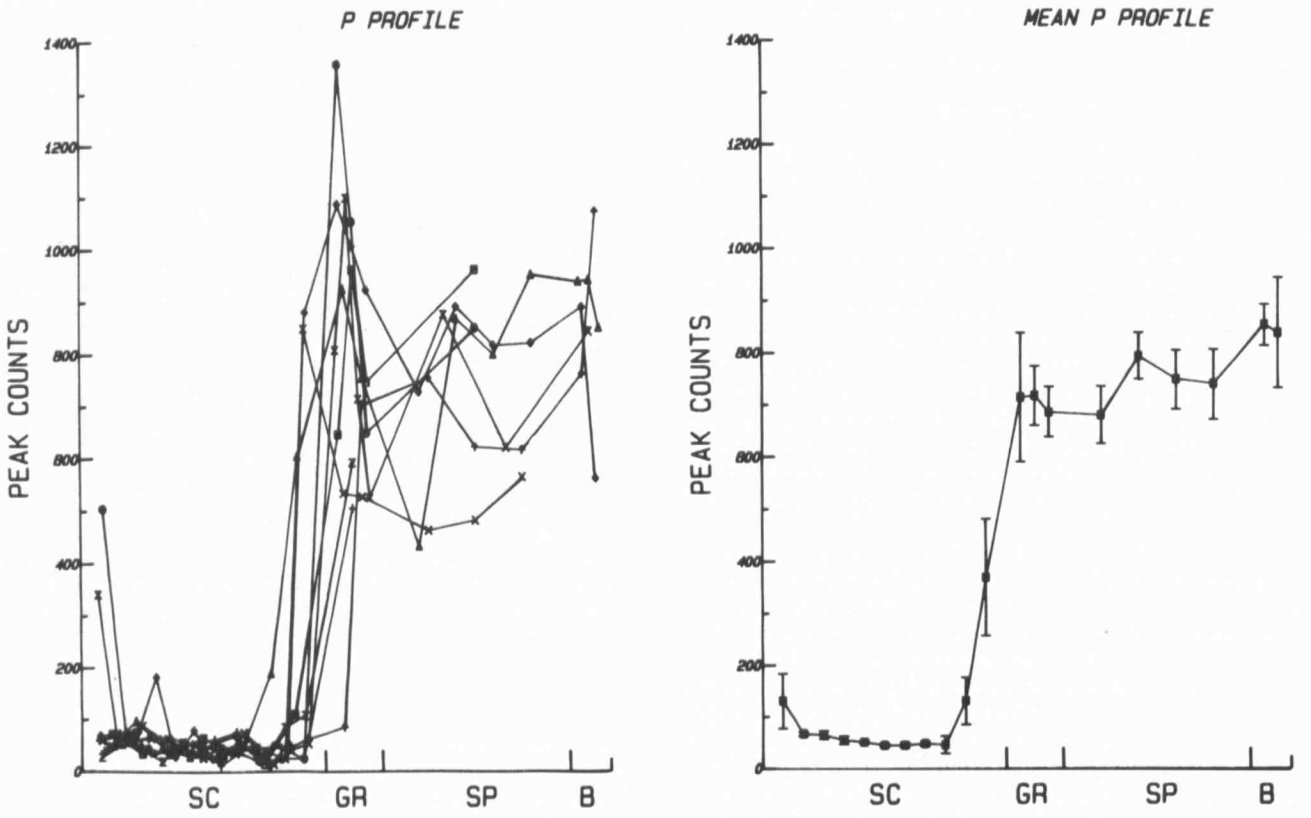

Figure 2. Profiles of phosphorus x-ray counts across human epidermis. The vertical axis is proportional to element content/unit volume. The horizontal axis denotes position within the tissue: *SC*, stratum corneum; *GR*, stratum granulosum; *SP*, stratum spinosum; *B*, basal layer. The widths of the morphological regions are not drawn to scale. Left graph: Each data point represents a single P measurement. Data points from individual profiles are connected by lines. Right graph: Profile of averaged P x-ray counts across human epidermis. Error bars represent standard errors of the mean. The large standard errors encountered in the viable tissue can likely be attributed to problems in normalizing the various P profiles to the very low counts in the inner stratum corneum.

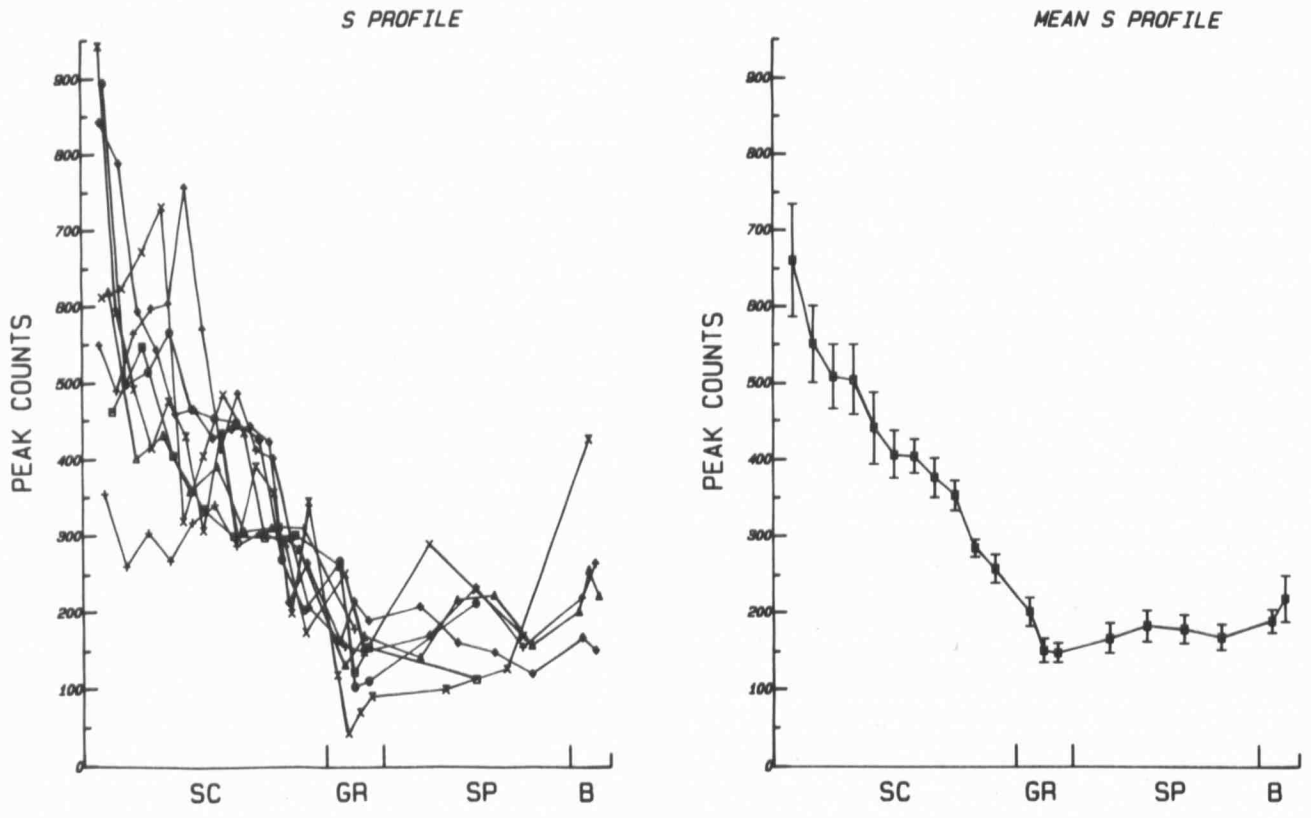

Figure 3. Profiles of sulfur x-ray counts across human epidermis. Axes are described in Fig 2. Left graph: Each data point represents a single S measurement. Data points from individual profiles are connected by lines. Right graph: Profile of averaged S x-ray counts across human epidermis.

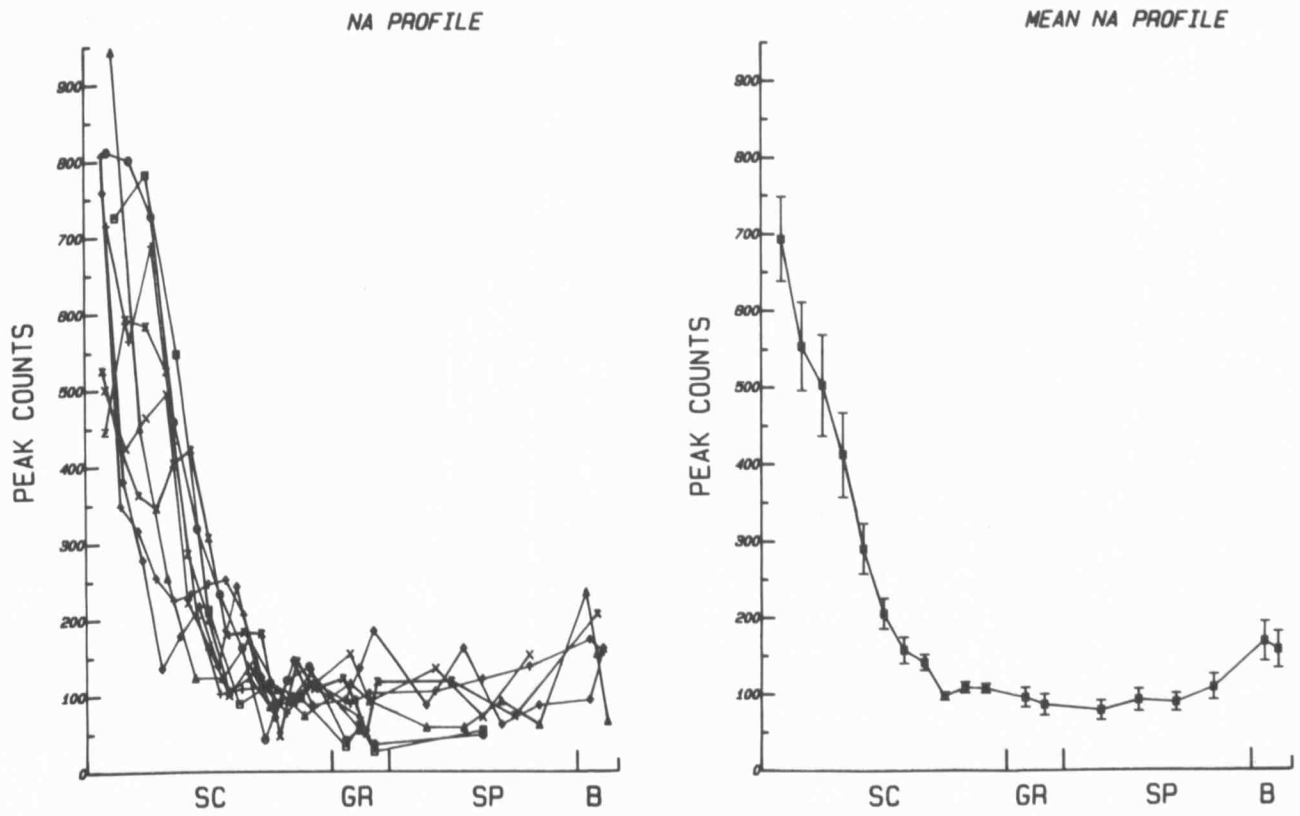

Figure 4. Profiles of sodium x-ray counts across human epidermis. Axes are described in Fig 2. Left graph: As before, each data point represents a single Na measurement, and data points from individual profiles are connected by lines. Right graph: Profile of averaged Na x-ray counts across human epidermis.

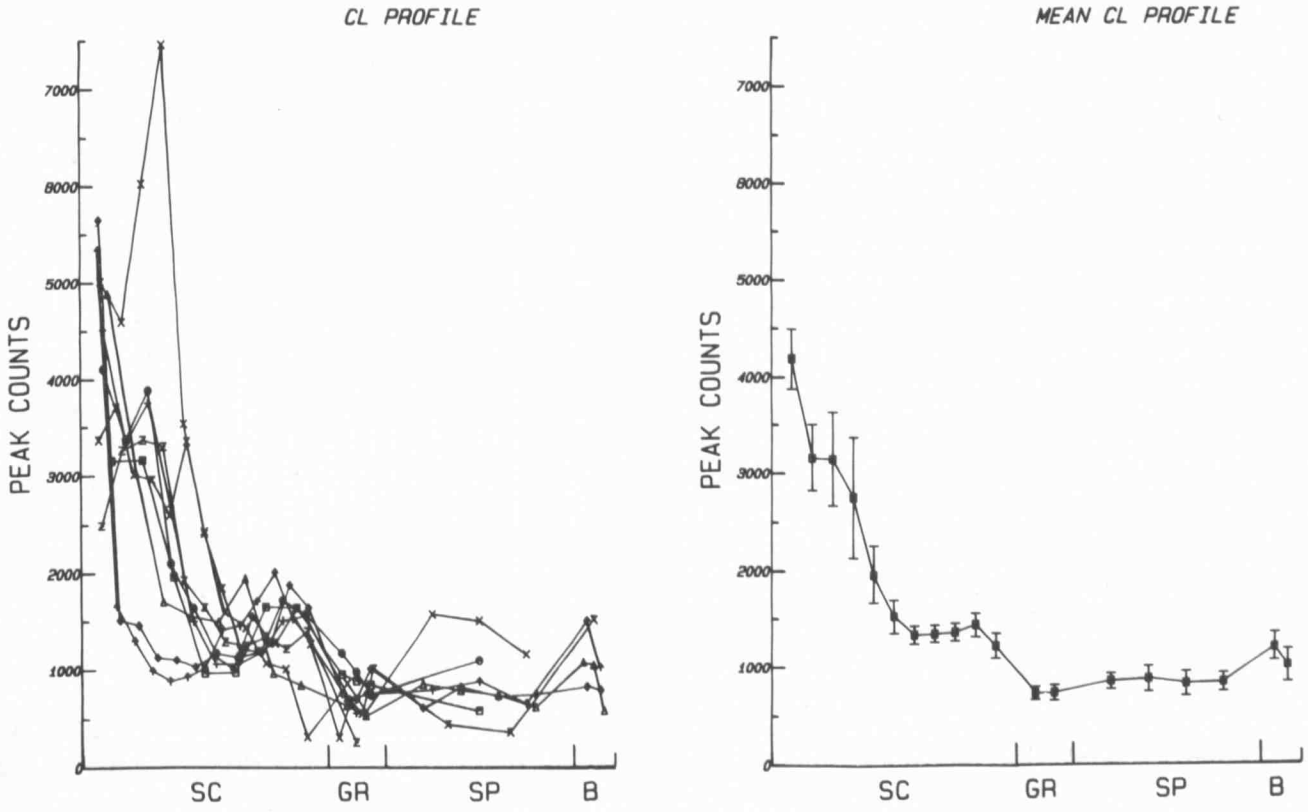

Figure 5. Profiles of chlorine x-ray counts across human epidermis. Axes are described in Fig 2. Left graph: Single data points for Cl from individual profiles are connected by lines. Right graph: Profile of averaged Cl x-ray counts across human epidermis.

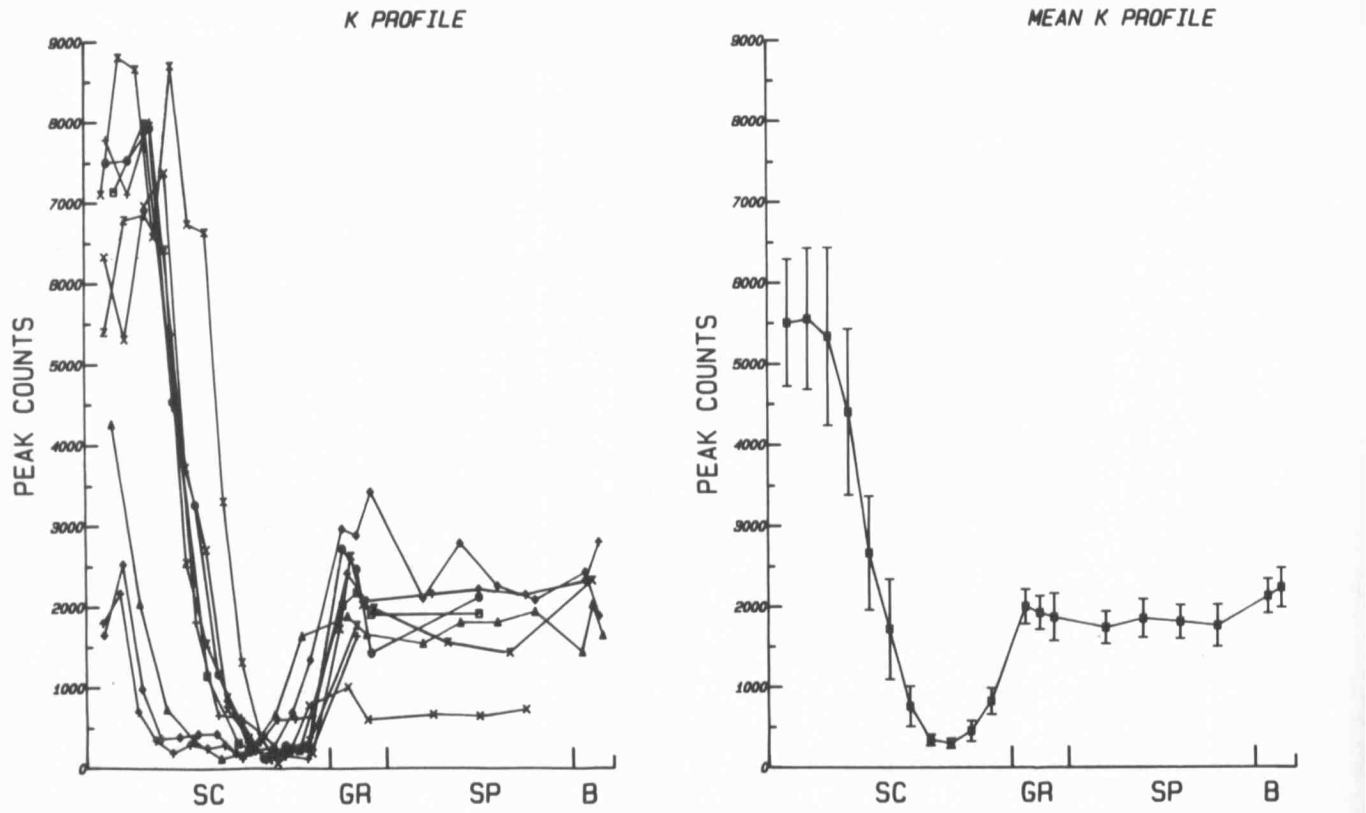

Figure 6. Profiles of potassium x-ray counts across human epidermis. Axes are described in Fig 2. Left graph: Single data points for K from individual profiles are connected by lines. Right graph: Profile of averaged K x-ray counts across human epidermis.

steep increase in Cl to a value approximately 6 times that of the viable tissue.

The K profile is shown in Fig 6. Like the other elements, K is constant throughout the viable tissue. Like P, there is a precipitous decrease in K to very low levels in the inner stratum corneum, although the drop in K is not always synchronous with the drop in P. Approximately mid-way through the stratum corneum there is a dramatic increase in K to values approximately 3 times that in the viable tissue. The large gradient for K in the outer half of the stratum corneum correlates well with the gradients for Na and Cl.

Element Profiles per Unit Mass of Tissue The previous Figs 2 to 6 expressed element profiles in terms of element content/unit volume. More commonly, electron probe data is expressed in terms of element content/unit dry weight [22–25,36,42]. Considering the large variation in dry mass encountered in skin [1], expressing results per unit dry weight can be misleading; nevertheless, reporting results in these units can provide useful perspectives to the data. Figure 7 shows the data for S from Fig 3 replotted per unit dry weight. The large S gradient across the stratum corneum in Fig 3 is now virtually eliminated. This is not the case for the more diffusible elements, and the large K, Na, and Cl gradients that occur from the middle of the stratum corneum to the outer surface (Figs 4 to 6, respectively) are preserved when the element distributions are replotted per unit dry weight, as shown in Fig 8.

DISCUSSION

Although all measurements reported in this and the accompanying paper [1] were obtained from the skin of a single individual, we have observed similar element and dry mass distributions in normal skin from other individuals (data not shown). We believe our results can be generalized.

The element profiles that we observe for S and P are supported by previous investigations. The near absence of P in stratum corneum cells was noted a decade ago [19], was inferred from biochemical

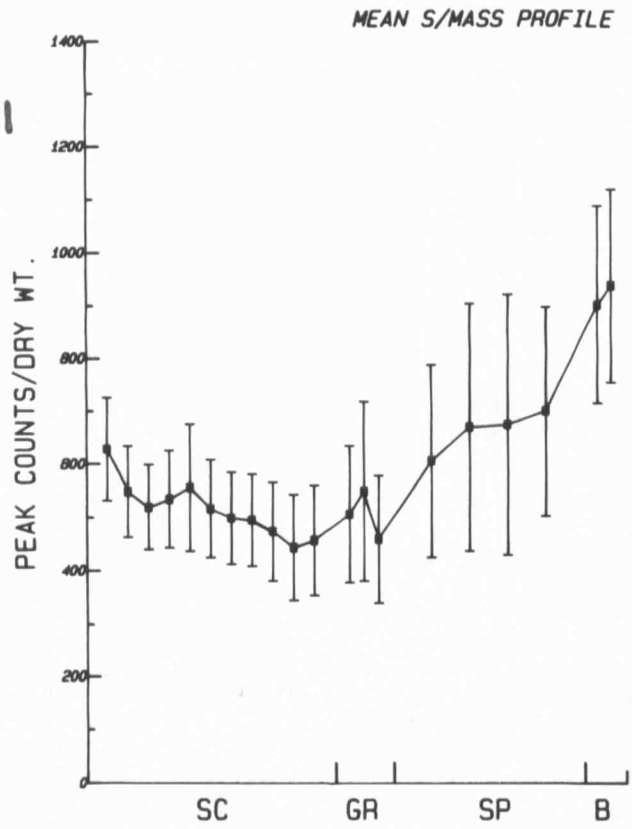

Figure 7. Averaged S/dry-wt profile (S peak counts/continuum x-ray counts at each point). The continuum x-ray count is proportional to dry mass. Ordinate, ×1000.

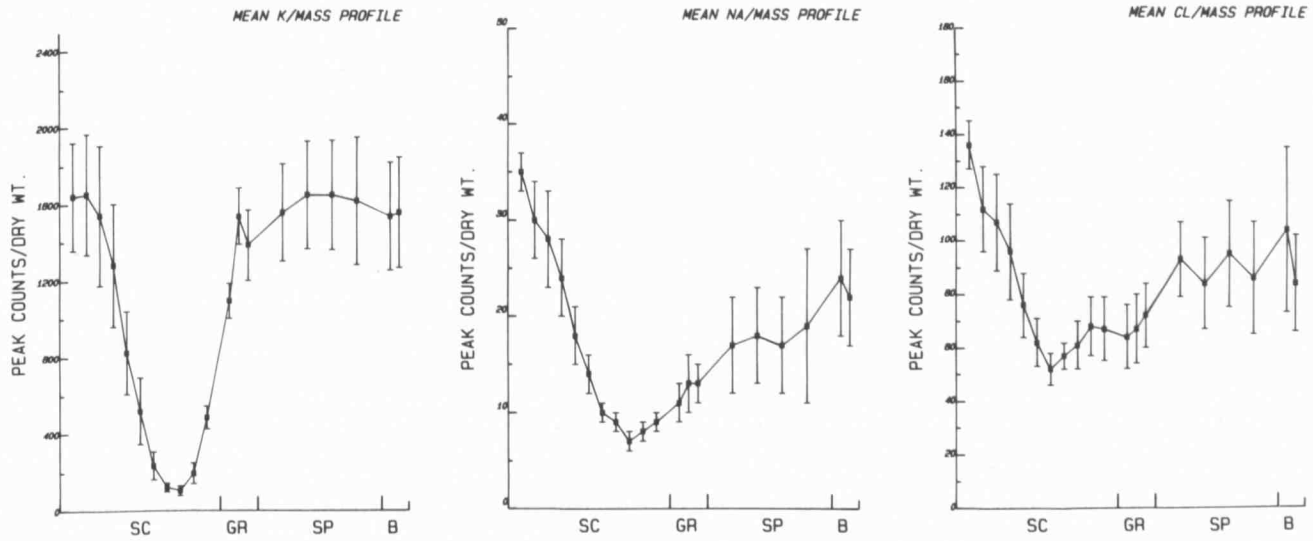

Figure 8. Averaged K, Na, and Cl profiles per unit dry weight (element peak counts/continuum x-ray counts at each point). K ordinate, ×1000; Na and Cl ordinate, ×100.

investigations [14–16], and was quantified in recent microprobe studies [22,25]. Our results in Fig 2 confirm the absence of P in this skin layer. The S distributions in Figs 3 and 7 are similar to previous microprobe studies [20,22,25,44].

Serious attempts to measure diffusible element distributions in mammalian skin have only recently appeared in the literatue [22–25]. Results from these pioneering microprobe studies on guinea pig and human skin are partly supported by our investigation. Consistent with our results, the previous studies found constant K and Cl concentrations throughout the stratum spinosum and basal layers [22,25]. Similarly consistent with our results, Cl levels were relatively unchanged in the inner stratum corneum (although in the previous studies this result was attributed to contamination), whereas K fell to low levels [22].

Although there are important similarities between our results and recent microprobe studies [22,25], there are equally important differences. In particular, differences occur in stratum granulosum concentrations, stratum corneum concentrations, and in the Na profile. Whereas the previous studies found a significant decline in Na, K, S, and P (but not Cl) concentrations per unit dry weight in the stratum granulosum [22,25], we observe little change in element concentrations per unit volume anywhere within the viable epidermal tissue (Figs 2 to 6) and little change in element concentrations per unit dry weight (Figs 7 and 8). In addition, the large concentration gradients that we observe in the outer stratum corneum were not described in the previous studies. Some discrepancies in results could be attributed to human vs. guinea pig differences. However, judging from the STEM micrograph of guinea pig skin published in one of the previous studies [22], the differences in results could be due to difficulties experienced by the previous authors in retaining the outer stratum corneum cell layers and in clearly distinguishing granular from stratum corneum cells. We are less able to explain the different Na profiles between some of the previous studies and our investigation. We found uniform Na values throughout the viable tissue, whereas the previous authors found higher Na values in spinosum compared to basal cells, resulting in a lower K/Na ratio within the spinosum [22]. The lower K/Na ratio was interpreted as an impairment of cellular metabolism or the beginning of cell death within the spinosum layer [22,44–46]. The hypothesis that spinosum cells are metabolically compromised has important implications for the understanding of keratinocyte differentiation. However, considerable variation in K/Na ratios in basal and spinosum layers have since been reported by this group. Values for K/Na in control tissue have ranged from 1.35 [45] to 3.68 [23], and the K/Na ratios in the spinosum have exceeded those in the basal layer in several instances [24,25]. Although it is not clear whether the previous observations on different K/Na ratios between cell layers are meaningful, our own observation of a uniform Na distribution in the viable epidermal tissue is not beyond reproach. Our estimate of the cellular Na concentration (moles/liter water) in viable tissue appears high to us (data not shown), and we can ɔt exclude the possibility that the anaesthetic used before biopsy has affected cellular Na levels. This possibility notwithstanding, we believe most of the data is compatible with Na concentrations (and indeed concentrations for all the elements studied) being uniform throughout the viable epidermal tissue.

Previous microprobe studies of frog skin [47,48] found uniform element concentrations throughout the viable tissue, similar to our results in the human and indicative of some commonality between the species. In the frog, the viable cells were shown to behave as a syncytium, with movement of electrolytes between the stratum granulosum and basal layer occurring via intercellular junctions [47,48]. Our data in no way proves the existence of a similar syncytium in the human, but our data and the presence of gap junctions in human epidermis [49,50] are compatible with a syncytial organization.

The towering gradients for S, K, Na, and Cl in the outer half of the stratum corneum (Figs 3 to 6) might be explained by simple water abstraction from the stratum corneum cells during transit, which would concentrate the intracellular solutes. Alternatively, the gradients could be due to a flow of solutes, either outward from the underlying tissues or inward from the skin surface. The first possibility can be directly investigated by expressing results per unit dry weight, as was done in Figs 7 and 8. As shown in Fig 7, the gradient for S is virtually eliminated, indicating that this gradient, or most of this gradient, can be attributed to water loss from the stratum corneum cells as they migrate outwards. However, for K, Na, and Cl, a large gradient still persists, indicating an addition of these elements has occurred per unit dry mass. The near absence of K from the inner half of the stratum corneum (Figs 6 and 8) suggests this element does not readily partition into the inner layer and makes it very unlikely that the large gradient in the outer stratum corneum could originate from the underlying tissue. The only reasonable explanation for the large K gradient is the inward diffusion of K from the skin surface. The source of this K is presumably sweat salts, a source that would readily account for the Na and Cl gradients as well. This process of sweat salt addition to the outer stratum corneum is shown in schematic form in the left portion of Fig 9. Although the primary function of sweat is thermoregulation [51], another possible function of sweat is the delivery of solute to the

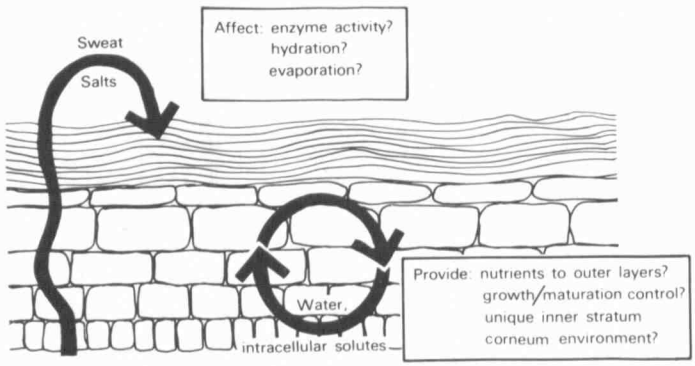

Figure 9. Proposed model of inorganic element cycles in human skin. Salts from sweat are delivered to the skin surface; carrier evaporation leaves high salt concentrations that diffuse into the outer stratum corneum. These solutes potentially affect enzyme activity, protein organization, and skin hydration. Within the viable tissue, K, P, and likely other intracellular solutes are recycled from transforming cells within the granular layer. These solutes potentially support metabolism in cell layers far removed from a nutrient source, participate in growth/maturation control, or simply by their exclusion from upper layers provide a unique environment within the inner stratum corneum.

outer stratum corneum. Since Na, K, and Cl are constituents of the "natural moisturizing factors" [52], these elements could play a role in skin conditioning. The high solute concentrations in the outer stratum corneum layers, estimated to be in the molar range, could reduce water activity in this region. The reduction in water activity would both increase water flux to the outer layers from within (hydration) yet decrease the "insensible" passive loss of water through evaporation. Alternatively, the high solute concentrations could affect enzyme activity; in particular, the swing in K from high levels at the skin surface to its virtual absence in the inner stratum corneum makes this element a particularly attractive candidate for controlling enzyme activation (such as might occur in desquamation).

Finally, our data highlights an important process that must be occurring within the viable epidermis. The sudden loss of P and K (and water [1]) at the stratum corneum-granulosum boundary suggests that for mass-balance to occur, these constituents must in some way be recycled within the viable tissue, as modeled in Fig 9. Although these important intracellular constituents could be released to the adjacent extracellular space, a syncytial organization of this tissue, mentioned earlier, would allow recycling completely within the intracellular compartment. Since the granular layer is thought to be responsible for formation of the primary (lipid) barrier in skin [53,54], the proper metabolic activity of this layer should be of some consequence. However, this layer is nearly 100 μm away from a capillary bed. This distance from a nutrient supply is large for a diffusional process and may constrain the adequate delivery of nutrients. A release of intracellular solutes from transforming granular cells would constitute a virtual nutrient source existing immediately underneath the stratum corneum. Alterations in this solute (and water) recirculation within the viable layer could play regulatory roles in the physiology of skin. The model in Fig 9 summarizes our observations on inorganic element movements within skin and highlights some of the questions these observations raise.

The authors wish to acknowledge helpful discussions with Dr. Vladimir Gartstein and Dr. Jerry Kasting.

REFERENCES

1. Warner RR, Myers MC, Taylor DA: Electron probe analysis of human skin: determination of the water concentration profile. J Invest Dermatol 90, 1987
2. Rothman S: Physiology and Biochemistry of the Skin. Chicago, Illinois, University of Chicago Press, 1954, pp 36–37
3. Tregear RT: The permeability of mammalian skin to ions. J Invest Dermatol 46:16–23, 1966
4. Wahlberg JE: Some attempts to influence the percutaneous absorption rate of sodium and mercuric chlorides in the guinea pig. Acta Dermatovenereol 45:335–343, 1965
5. Scheuplein RJ, Blank IH: Permeability of the skin. Physiol Rev 51:702–747, 1971
6. Grice K, Sattar H, Baker H: The cutaneous barrier to salts and water in psoriasis and in normal skin. Br J Dermatol 88:459–463, 1973
7. Grice K, Sattar H, Casey T, Baker H: An evaluation of Na^+, Cl^-, and pH ion-specific electrodes in the study of the electrolyte contents of epidermal transudate and sweat. Br J Dermatol 92:511–518, 1975
8. Rothman S: Physiology and Biochemistry of the Skin. Chicago, IL, University of Chicago Press, 1954, pp 9–25
9. Leveque JL, De Rigal J: Impedance methods for studying skin moisturization. J Soc Cosmet Chem 34:419–428, 1983
10. Barker AT, Jaffe LF, Vanable JW Jr: The glabrous epidermis of cavies contains a powerful battery. Am J Physiol 242:R358–R366, 1982
11. France VM: Active sodium uptake by the skin of foetal sheep and pigs. J Physiol (Lond) 258:377–392, 1976
12. Rudall KM: The proteins of the mammalian epidermis. Adv Protein Chem 7:253–290, 1952
13. Van Scott EJ, Flesch P: Sulphydryl and disulphide groups in keratinisation. Science (Wash DC) 119:70–71, 1954
14. Long VJW: Variation in lipid composition at different depths in the cow snout epidermis. J Invest Dermatol 55:269–273, 1970
15. Gray GM, Yardley HJ: Different populations of pig epidermal cells: isolation and lipid composition. J Lipid Res 16:441–447, 1975
16. Lonsdale-Eccles JD, Haugen JA, Dale BA: A phosphorylated keratohyalin-derived precursor of epidermal stratum corneum basic protein. J Biol Chem 255:2235–2238, 1980
17. King CS, Moore N, Marks R, Nicholls S: Preliminary studies into percorneal penetration and elemental content of the stratum corneum using X-ray microanalysis. Arch Dermatol Res 263:257–265, 1978
18. Suderman DR, Cunningham FE: Detection of elements in poultry skin by energy dispersive analysis of X-rays with the scanning electron microscope. Poultry Sci 58:1224–1227, 1979
19. Jessen H, Peters PD, Hall TA: Sulfur in epidermal keratohyalin granules: a quantitative assay by x-ray microanalysis. J Cell Sci 22:161–171, 1976
20. Sims RT, Hall T: X-ray emission microanalysis of proteins and sulphur in rat plantar epidermis. J Cell Sci 3:563–572, 1968
21. Burkhart CG, Burnham JC: Elevated phosphorus in psoriatic skin determined by energy dispersive x-ray micro-analysis. J Cutaneous Pathology 10:171–177, 1983
22. Wei X, Roomans GM, Forslind B: Elemental distribution in guinea-pig skin as revealed by x-ray microanalysis in the scanning transmission microscope. J Invest Dermatol 79:167–169, 1982
23. Lindberg M, Roomans GM: Elemental redistribution and ultrastructural changes in guinea pig epidermis after dinitrochlorobenzene (DNCB) exposure. J Invest Dermatol 81:303–308, 1983
24. Lindberg M, Forslind B, Roomans GM: Elemental changes at irritant reactions due to chromate and nickel in guinea-pig epidermis, in Scanning Electron Microscopy/1983/III. Edited by O Johari. AMF O'Hare, Chicago, SEM INC., 1983, pp 1243–1247
25. Grundin TG, Roomans GM, Forslind B, Lindberg M, Werner Y: X-ray microanalysis of psoriatic skin. J Invest Dermatol 85:378–380, 1985
26. Menon GK, Grayson S, Elias PM: Ionic calcium reservoirs in mammalian epidermis: ultrastructural localization by ion-capture cytochemistry. J Invest Dermatol 84:508–512, 1985
27. Cone CD Jr: Unified theory on the basic mechanism of normal mitotic control and oncogenesis. J Theor Biol 30:151–181, 1971
28. Rozengurt E, Mendoza S: Monovalent ion fluxes and the control of cell proliferation in cultured fibroblast. Ann NY Acad Sci 339:175–189, 1980
29. Hennings H, Michael D, Cheng C, Steinert P, Holbrook K, Yuspa SH:

Calcium regulation of growth and differentiation of mouse epidermal cells in culture. Cell 19:245–254, 1980

30. Rothenberg P, Glaser L, Schlesinger P, Cassel D: Activation of Na^+/H^+ exchange by epidermal growth factor elevates intracellular pH in A431 cells. J Biol Chem 258:12644–12653, 1983
31. Rosoff PM, Cantley LC: Ion fluxes and differentiation in transformed cell lines, in Regulation and Development of Membrane Transport Processes. Edited by JS Graves. New York, John Wiley, 1985, pp 194–204
32. Rice RH, Green H: Presence in human epidermal cells of a soluble protein precursor of the cross-linked envelope: activation of the cross-linking by calcium ions. Cell 18:681–694, 1979
33. Dale BA, Schofield JAH, Hennings H, Stanley JR, Yuspa SH: Identification of filaggrin in cultured mouse keratinocytes and its regulation by calcium. J Invest Dermatol 81:90–95, 1983
34. Somero GN: Protons, osmolytes, and fitness of internal milieu for protein function. Am J Physiol 25:R197–R213, 1986
35. Warner RR, Myers MC, Taylor DA: Localization of diffusible elements and water in skin. J Invest Dermatol 84:301, 1985
36. Somlyo AV, Shuman H, Somlyo AP: Elemental distribution in striated muscle and effects of hypertonicity; electron probe analysis of cryosections. J Cell Biol 74:828–857, 1977
37. Lechene CP, Warner RR: Ultramicroanalysis: x-ray spectrometry by electron probe excitation. Ann Rev Biophys Bioeng 6:57–85, 1977
38. Dörge A, Rick R, Gehring K, Thurau K: Preparation of freeze-dried cryosections for quantitative X-ray microanalysis of electrolytes in biological soft tissues. Pflügers Arch 373:85–97, 1978
39. Gupta BL, Hall TA, Moreton RB: Electron probe X-ray microanalysis, in Transport of Ions and Water in Animals. Edited by BL Gupta, RB Moreton, JL Oschman & BJ Wall. New York, Academic Press, 1977, pp 83–143
40. Warner RR, Myers MC, Taylor DA: Inaccuracies with the Hall technique due to continuum variation in the analytical microscope. J Microsc 138:43–52, 1985
41. Myers MC, Warner RR: A routine procedure for monitoring sample mass during microanalysis, in Microbeam Analysis—1985. Edited by JT Armstrong. San Francisco, San Francisco Press, 1985, pp 129–131
42. Hall TA: The microprobe assay of chemical elements, in Physical Techniques in Biological Research. Edited by G Oster. 2nd edition, Vol. 1A, New York, Academic Press, 1971, pp 157–275
43. Hagler HK, Buja LM: Effect of specimen preparation and section transfer techniques on the preservation of ultrastructure, lipids and elements in cryosections. J Microsc 141:141–152, 1986
44. Forslind B, Wei X, Roomans GM: Elemental distribution in cross sections of guinea-pig epidermis: x-ray microanalysis in the electron microscope, in Stratum Corneum. Edited by R Marks & G Plewig. New York, Springer-Verlag, 1983, pp 217–220
45. Forslind B: X-ray microanalysis in dermatology, in Scanning Electron Microscopy/1982/IV. Edited by O Johari. AMF O'Hare, Chicago, SEM Inc., 1982, pp 1715–1724
46. Forslind B: Clinical applications of scanning electron microscopy and x-ray microanalysis in dermatology, in Scanning Electron Microscopy/1984/I. Edited by O Johari. AMF O'Hare, Chicago, SEM Inc., 1984, pp 183–206
47. Rick R, Dörge A, Von Arnim E, Thurau K: Electron microprobe analysis of frog skin epithelium: evidence for a syncytial sodium transport compartment. J Memb Biol 39:313–331, 1978
48. Rick R, Dörge A, Thurau K: Electron microprobe analysis of frog skin epithelium: pathway of transepithelial sodium transport, in Ion Transport by Epithelia. Edited by SG Schultz. New York, Raven Press, 1981, pp 197–208
49. Elias PM, McNutt NS, Friend DS: Membrane alterations during cornification of mammalian squamous epithelia: a freeze-fracture, tracer, and thin-section study. Anat Rec 189:577–594, 1977
50. Caputo R, Peluchetti D: The junctions of normal human epidermis: a freeze-fracture study. J Ultrastruct Res 61:44–61, 1977
51. Medical Physiology. Edited by VB Mountcastle. St. Louis, CV Mosby Co, Vol. 2, 13th edition, 1974, P 1319
52. Jacobi OK: Moisture regulation in the skin. Drug Cosmet Ind 84:732–733, 810–812, 1959
53. Elias PM, Friend DS: The permeability barrier in mammalian epidermis. J Cell Biol 65:180–191, 1975
54. Elias PM, Cooper ER, Korc A, Brown BE: Percutaneous transport in relation to stratum corneum structure and lipid composition. J Invest Dermatol 76:297–301, 1981